


**Possible continuous transition from fractional quantum Hall to stripe phase at  $\nu_e = 7/3$** Prashant Kumar<sup>1</sup> and R. N. Bhatt<sup>2</sup><sup>1</sup>*Department of Physics, Princeton University, Princeton, New Jersey 08544, USA*<sup>2</sup>*Department of Electrical and Computer Engineering, Princeton University, Princeton, New Jersey 08544, USA* (Received 24 May 2022; revised 15 August 2022; accepted 25 August 2022; published 1 September 2022)

We study the phase diagram of the  $\nu_e = 7/3$  state in the  $N = 1$  Landau level in the presence of band mass anisotropy. Using the density matrix renormalization group on an infinite cylinder geometry, we find a continuous transition from the topologically ordered Laughlin fractional quantum Hall state to a stripe phase with a period of approximately five and a half magnetic lengths. The transition is driven by the condensation of the magnetoroton mode which becomes gapless at the critical point. We interpret the transition within the composite-boson theory as the onset of stripe order in a superfluid background, resulting from the roton mode going soft.

DOI: [10.1103/PhysRevB.106.115101](https://doi.org/10.1103/PhysRevB.106.115101)**I. INTRODUCTION**

A two-dimensional electron gas in a large perpendicular magnetic field exhibits a rich set of phenomena dominated by strong correlations between the electrons. If the applied magnetic field is strong, the electrons are essentially confined to Landau levels (LLs), with an integer number of filled LLs plus one fractionally filled LL at the top determined by the total filling fraction  $\nu_e$ . Since filled LLs give rise only to a quantized Hall conductance and are inert otherwise, this makes the interaction the sole term in the low energy Hamiltonian. The fractional quantum Hall (FQH) effect is a spectacular consequence of such interaction driven physics in the lowest few LLs.

An interesting question that arises is what phase transitions may occur between the FQH and other stable phases. In the presence of disorder, integer and fractional quantum Hall transitions are well known examples. Further, spontaneous nematic order may occur in higher LLs [1–7]. In this paper, we find numerical evidence for a continuous transition from the Laughlin FQH to the stripe phase at  $\nu_e = 7/3$ , when the Hamiltonian is translationally invariant but breaks the rotational symmetry.

The FQH states in  $N = 1$  LL have smaller gaps and are in general more susceptible to perturbations compared to the ones in the lowest LL [8–11]. In previous numerical studies, band anisotropy has been proposed to destabilize the FQH state in favor of a spontaneously broken translational symmetry state, in particular the stripe phase [9,12–17]. However, the nature of such a transition is unclear. Motivated by this, we study the phase diagram of  $\nu_e = 7/3$  state as a function of anisotropy in the  $N = 1$  LL in the presence of Coulomb interactions.

We use the density matrix renormalization group on an infinite cylinder geometry (iDMRG) projected to the  $N = 1$  LL to study the effects of anisotropy [18,19]. By computing observables such as the correlation length, magnetoroton gap, and the stripe order parameter, we show that the transition from the Laughlin FQH state to the stripe phase is continuous.

The transition is driven by the condensation of the magnetoroton at a finite wave vector and it becomes gapless at criticality. We note that a continuous transition from a Wigner crystal to the stripe phase has been proposed to take place in the  $N = 2$  LL Ref. [17].

In the Landau gauge, the onset of this phase is characterized by an  $n$ -fold increase in the periodicity of the Laughlin state and thus corresponds to the spontaneous breaking of  $Z_n$  symmetry. It is found that  $n$  increases with the circumference of the cylinder such that the period of the stripe phase remains unchanged when expressed in the units of magnetic length.

The FQH and the stripe phase appear to be unrelated at first glance and a continuous transition between the two seems puzzling. We propose that the critical point may be understood from the perspective of the composite-boson (CB) theory [20]. The stripe phase can occur via the condensation of the roton mode of the CB superfluid and the transition can be second order.

This paper is organized as follows. In Sec. II, we explain the model and the methods used to observe the FQH to stripe phase transition in iDMRG. We present evidence to support our claim that the transition is second order in Sec. III and determine the critical exponents on the infinite cylinder geometry for the  $Z_2$ ,  $Z_3$ , and  $Z_4$  cases. We comment on the relation between the critical point in the quasi-one-dimensional (quasi-1D) ‘geometry and  $Z_n$  chiral clock models in Sec. IV. The composite-boson interpretation of the transition is discussed in Sec. V. We summarize our findings and give concluding remarks in Sec. VI.

**II. MODEL AND METHODS**

Let us consider electrons in two dimensions interacting via a density-density interaction in the presence of a uniform perpendicular magnetic field  $B$ . In the limit when the interaction is weak compared to the cyclotron energy, it is sufficient to project to the highest energy LL that is partially filled. In this

paper, we are interested in the  $N = 1$  LL. The electrons can be described by the following Hamiltonian:

$$H = \frac{1}{2} \int \frac{d^2q}{(2\pi)^2} V(\mathbf{q}) f(\mathbf{q})^2 : \bar{\rho}(\mathbf{q}) \bar{\rho}(-\mathbf{q}) :, \quad (1)$$

$$\bar{\rho}(\mathbf{q}) = \sum_j e^{-i\mathbf{q}\cdot\mathbf{R}_j}, \quad (2)$$

where  $\ell^2 = 1/B$  is the magnetic length,  $V(\mathbf{q})$  is the interaction potential,  $\bar{\rho}(\mathbf{q})$  is the guiding center density operator and  $f(\mathbf{q})$  is the form factor of the  $N = 1$  LL. Further,  $\mathbf{R}_j$  are the guiding center coordinates of the  $j$ th particle. They are defined as  $R^\alpha = r^\alpha + \ell^2 \epsilon^{\alpha\beta} \Pi_\beta$  and satisfy the commutation relation  $[R^\alpha, R^\beta] = -i\ell^2 \epsilon^{\alpha\beta}$ . Also, the kinetic momentum is  $\Pi_\alpha \equiv p_\alpha - A_\alpha$ , where  $p_\alpha$  is the canonical momentum and  $A_\alpha$  is the electromagnetic vector potential.

In our iDMRG simulations, we use an infinite cylinder geometry with its axis aligned along the  $y$  direction and the periodic circumference direction along the  $x$  axis. We consider the Landau gauge defined by the vector potential  $\mathbf{A} = -By\hat{x}$ . As a consequence of the translational invariance along  $x$  direction, the single-particle wave functions have the form  $\psi_k(\mathbf{r}) \propto e^{ikx} g(y + k\ell^2)$ . Periodic boundary conditions along the circumference lead to  $k = \kappa n$ , where  $\kappa \equiv 2\pi/L_x$ ,  $L_x$  is the circumference of the cylinder and  $n \in \mathbb{Z}$ . Therefore, the LL orbitals in the Landau gauge form a 1D lattice with sites spaced by  $2\pi/L_x$ . The guiding center density and the Hamiltonian can be expressed in a second quantized form as follows:

$$\bar{\rho}(q_x, q_y) = \delta_{q_x, \kappa k} e^{ickq_y/2} \sum_n e^{icknq_y} c_n^\dagger c_{n+k}, \quad (3)$$

$$H = \frac{1}{2} \sum_{nmk} V_{mk} c_n c_{n+k}^\dagger c_{n+m}^\dagger c_{n+m+k}, \quad (4)$$

$$V_{mk} = \frac{1}{L_x} \int \frac{dq_y}{2\pi} V(\kappa k, q_y) f(\kappa k, q_y)^2 e^{ickmq_y}, \quad (5)$$

where  $n, m, k \in \mathbb{Z}$  and only the antisymmetric component of  $V_{mk}$  (under  $m \leftrightarrow k$ ) is important.

We introduce band anisotropy by considering an anisotropic mass tensor diagonal in the basis defined by the coordinate axes. To be precise, the kinetic energy has the following form before projection to the  $N = 1$  LL:

$$H_{K.E.} = \frac{\Pi_x^2}{2m\alpha} + \frac{\alpha \Pi_y^2}{2m}, \quad (6)$$

where  $\alpha$  is a measure of the mass anisotropy. The Hamiltonian when projected to the  $N = 1$  LL leads to an anisotropic form factor given by

$$f(\mathbf{q}) = \left( 1 - \frac{|q'|^2 \ell^2}{2} \right) e^{-|q'|^2 \ell^2 / 4}, \quad (7)$$

where  $q' \equiv q_x/\sqrt{\alpha} + i\sqrt{\alpha}q_y$ .

In this paper, we assume that the electrons repel each other via isotropic Coulomb interactions, i.e.,

$$V(\mathbf{r}) = \frac{e^{-r^2/2\xi^2}}{r}, \quad (8)$$

where we have regulated the interaction at long distances using a Gaussian factor with a width equal to  $\xi$ . We take

$\xi = 6\ell$ , which was found to not cause any significant effect in previous work [21].

### A. Observing the stripe phase in quasi-1D geometry

In previous iDMRG simulations, the ground state at  $\nu_e = 7/3$ , in the presence of an isotropic Coulomb potential, has been found to be the Laughlin FQH state with a longer correlation length compared to  $\nu_e = 1/3$  [19]. Therefore, unlike  $\nu_e = 1/3$  [8], it could be more susceptible to a phase change. As we show later, the magnetoroton gap collapses upon increasing the band anisotropy and the system undergoes a phase transition to a stripe phase.

We observe the stripe phase in iDMRG as follows. In the infinite matrix-product state (iMPS) form, the Laughlin FQH ground state at  $\nu_e = 7/3$  is found in the root configuration 010 [22,23]. This implies that the ground state on the infinite cylinder can be constructed by repeating a unit cell MPS composed of three orbitals with the same quantum numbers as the electron configuration 010. If the stripes in the stripe phase are parallel to the  $x$  axis and its period contains  $3n$  number of Landau orbitals, the translational symmetry of the Laughlin state is broken “ $n$ -fold.” The transition to the ordered phase can then be observed by computing the ground state iMPS with a unit cell containing  $3n$  orbitals at various values of anisotropy.

On the infinite cylinder, we denote the stripe order as  $Z_n$ . In general,  $n$  depends on the circumference. It is found that  $n = \mathcal{O}(L_x/\ell)$ , so that, in the units of magnetic lengths, the period  $a_0 = 3n \times 2\pi\ell^2/L_x$  remains roughly constant as we increase the cylinder circumference. This indicates that the stripe phase is not a finite-size artifact and is relevant to the 2D physics.

Our strategy for computing the ground state is as follows. We initialize the iMPS and environments with an electron configuration  $0_n 1_n 0_n$ , introducing an initial  $Z_n$  stripe order. Here, the subscript denotes an  $n$ -fold repetition of the electron occupation number. Notice that this has the same quantum numbers as the configuration  $(010)_n$  of the Laughlin FQH state. As we perform the iDMRG steps, strength of the stripe order parameter decays to zero (nonzero) if the system is in the FQH (stripe) state. We found good convergence with independent simulations at each anisotropy in the stripe phase. On the FQH side, we find that the best convergence and lowest energies are obtained if one starts in the FQH phase away from the transition and uses the converged ground state as an initial guess for a point closer to the transition. The ground state is thus adiabatically evolved as one moves towards the transition.

### B. Observables and critical scaling analysis

Near the quantum phase transition, we measure observables and perform a critical scaling analysis. In particular, we measure three quantities. First, the correlation length  $\xi$  is calculated directly from the MPS form of the ground state using its transfer matrix [24]. In general, all correlations decay faster compared to this length scale. We find that it is close to the one obtained by fitting the density-density correlation function to an exponentially decaying function.

TABLE I. Critical exponents for the FQH to stripe phase transitions on an infinite cylinder.

Symmetry	$\nu$	$\nu z$	$\beta$
$Z_2$	1.04	0.90	0.119
$Z_3$	0.87	0.69	0.109
$Z_4$	0.86	0.66	0.08

Second, we calculate the order parameter  $\rho_G$  by measuring the density profile along the axial direction of the cylinder and then taking a Fourier transform at the ordering wave vector  $\mathbf{G} = (0, 2\pi/a_0)$ . Third, the magnetoroton gap  $\omega_{\text{SMA}}$  at  $\mathbf{q} = \mathbf{G}$  is measured using the single-mode approximation (SMA) of Girvin, Macdonald, and Platzman [25]. While it is possible that SMA breaks down due to interactions between the gapless density fluctuations, it provides an energy scale for the critical fluctuations [26]. As such, it can be useful for studying dynamical scaling near the critical point.

We fit the three observables to power laws to obtain the critical exponents  $\nu$ ,  $\beta$ , and  $\nu z$  that correspond to the correlation length, order parameter strength, and energy gap exponents respectively [27].

The iMPS obtained in iDMRG is an approximation of the true ground state. This is so because the iMPS truncates the infinite-dimensional Hilbert space of the cylinder to a finite one characterized by the bond dimension  $\chi$ . One expects the observables to converge to the  $\chi \rightarrow \infty$  case as  $\chi$  is increased. However, we find that they do not show a numerically predictable behavior as a function of  $\chi$ . Therefore, we use the the largest  $\chi$  we can access to perform the critical scaling analysis. We find that the finite bond dimension affects the phase diagram in mainly two ways. First, the stripe phase is preferred since it has a lower entanglement entropy. Second, an iMPS with a finite bond-dimension cannot have an infinite correlation length and a continuous transition becomes weakly first order. Fortunately, even though the observables show such dependence on  $\chi$ , the critical exponents are not altered significantly.

### III. LAUGHLIN FQH TO STRIPE PHASE TRANSITION AT $\nu_e = 7/3$

In this section, we present our numerical results for the quantum phase transition from the  $\nu_e = 7/3$  Laughlin FQH state to the stripe phase as a band anisotropy is introduced in the system. We find that the transition is continuous, i.e., the inverse correlation length, energy gap, and order parameter go to zero at the critical point. As is evident in Fig. 1, it is driven by the condensation of the magnetoroton, which becomes gapless at criticality. In Fig. 2, we present the numerical results for the  $Z_2$ ,  $Z_3$ , and  $Z_4$  cases of the transition. The exponents  $\nu$ ,  $\nu z$ , and  $\beta$  are obtained by fitting the inverse correlation length, magnetoroton gap, and order parameter to power laws respectively. Their values are reported in Table I. These should be interpreted as effective exponents rather than the asymptotic ones [28]. Further, the energy gap exponent  $\nu z$  depends on the validity of the SMA. For the  $Z_4$  case, we find that the bond dimensions accessible to our numerical simulations are not

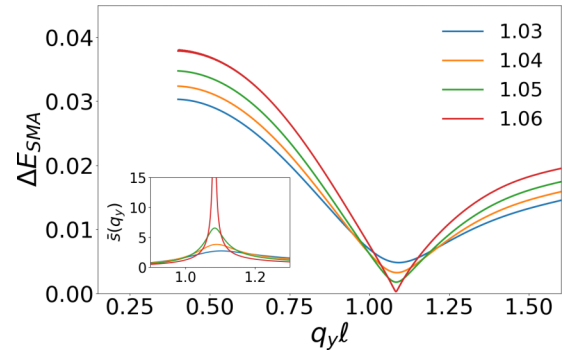


FIG. 1. The magnetoroton spectrum computed using the single-mode approximation (SMA) [25] for various values of anisotropy  $\alpha$  (as indicated in the figure),  $L_x = 6.5\ell$ , and  $q_y\ell = 0$ . The SMA energy goes to zero at  $q_y\ell = L_x/6\ell$  as the anisotropy is increased. This indicates the onset of stripe ordering with a period that contains six Landau orbitals in the  $y$  direction. The inset shows the divergence of the static structure factor  $\bar{s}(q_y)$  as one approaches the transition.

sufficient to perform a reliable critical scaling analysis [29]. In particular, the correlation lengths are not large enough to avoid finite size effects that come from the finite cylinder circumference and interaction range. Nevertheless, we have indicated the exponents as obtained from the fitting procedure.

As mentioned in Sec. II A, generally,  $n = \mathcal{O}(L_x/\ell)$ . We find that the commensurate stripe phase is strongest when the relation  $L_x \approx (3.5n - 0.5)\ell$  is satisfied. Thus, we obtain the period of the stripe phase to be  $a_0 \approx 5.4\ell$ .

### IV. QUASI-1D CRITICAL POINT AND $Z_n$ CHIRAL CLOCK MODELS

Across the transition, the translation symmetry is spontaneously broken  $n$ -fold on the quasi-1D cylindrical geometry. We expect such a critical point to be described by the  $Z_n$  chiral clock model [30–34]. To see this explicitly, note that the different  $Z_n$  stripe root configurations, for example  $1_30_30_3$ ,  $0_31_30_3$ , and  $0_30_31_3$  in the  $Z_3$  case, can be mapped to  $n$  number of states of a clock model. In general, a domain wall configuration, that moves the clock clockwise when moving to the right, has a different energy compared to when the clock moves anticlockwise. Thus, the  $Z_n$  clock model is chiral [34].

Another way to see how the chirality arises is in terms of the discrete symmetries. The Hamiltonian of Eq. (4) has two discrete symmetries. First, there is an antiunitary symmetry constructed by combining time reversal with the mirror transformation that leaves the  $y$  axis invariant. Additionally, we have an inversion symmetry which corresponds to a  $180^\circ$  rotation of the quasi-1D cylinder. In the language of clock models [33], the first discrete symmetry corresponds to time reversal while the second symmetry corresponds to the combination of charge conjugation and parity. Note that the charge conjugation and parity symmetries are broken individually in our problem, which leads to the aforementioned chirality in the  $Z_n$  clock model [34]. In this sense, the  $n$ -state Potts model which preserves all three discrete symmetries, i.e. charge conjugation, parity, and time reversal, is achiral.

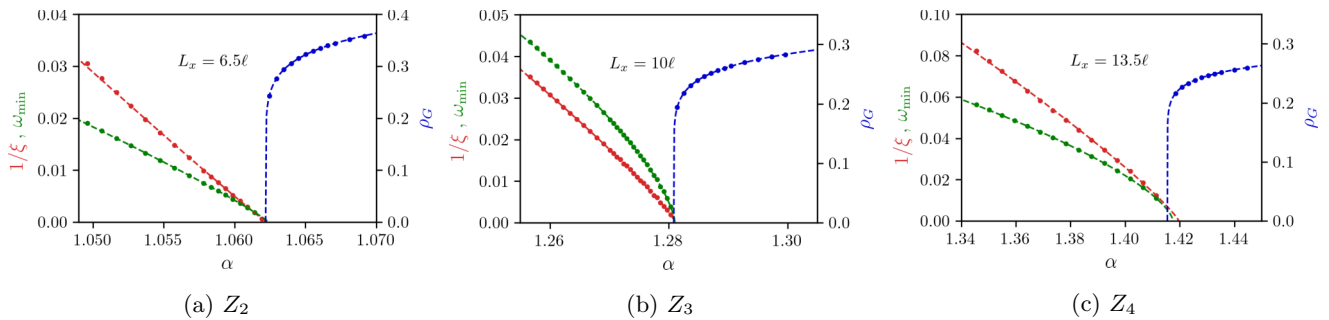


FIG. 2. Inverse correlation length  $1/\xi$  (red), SMA energy at the ordering wave vector,  $\omega_{\text{SMA}}$ , scaled up by an appropriate factor (green), and order parameter  $\rho_G$  (blue) for Laughlin FQH to (a)  $Z_2$ , (b)  $Z_3$ , and (c)  $Z_4$  stripe phase transitions on an infinite cylinder. By fitting the three quantities to a power law, we obtain the exponents  $(\nu, \nu z, \beta)$ : (a) (1.04, 0.90, 0.119), (b) (0.87, 0.69, 0.109), and (c) (0.86, 0.66, 0.08). The bond dimensions  $\chi$  are (a) 512, (b) 4096, and (c) 8192. The fitted curves meet at a single point for  $Z_2$  and  $Z_3$  cases, indicating a continuous transition. The appearance of a weakly first-order transition in the  $Z_4$  case may be due to stronger finite-size and bond-dimension effects.

Before comparing our results with the  $Z_n$  clock models, we mention an important caveat. The Hamiltonian of Eq. (4) has an additional conservation law that restricts the domain wall configurations and may change the universality class. To see this, let us consider a thin torus geometry with  $\ell \lesssim L_x \ll L_y$ . The root configuration for the Laughlin FQH state is given by  $(010)_{N_e}$ , where  $N_e$  is the number of electrons in the  $N = 1$  LL. In the Landau gauge, the total momentum along  $x$  direction is conserved modulo  $\kappa N_\phi$ , where  $N_\phi = 3N_e$ . Thus, the momentum is

$$P_x/\kappa = \left( \sum_{k=0}^{N_\phi-1} kn_k \right) \text{ mod } N_\phi. \quad (9)$$

$n_k \equiv c_k^\dagger c_k$  is the occupation number operator of the  $k^{\text{th}}$  orbital. Notice that the conservation of  $P_x$  is equivalent to the conservation of center of mass along the  $y$  direction.

Assuming  $N_e/n \in \mathbb{Z}$ , there are  $n$  degenerate ground states with the same total momentum  $P_x$  in the stripe phase. These correspond to the stripe pattern  $(0_n 1_n 0_n)_{N_e/n}$  and the ones generated when it is translated by  $3m$  Landau orbitals, where  $m \in \{1, 2, \dots, n-1\}$ . The domain walls between different ground states condense as one approaches the transition from the stripe phase side towards the FQH side. However, an arbitrary domain wall between two stripe patterns generally changes the position of the center of mass of electrons. Only a smaller set of configurations that respect the conservation law are allowed. At present, we are not aware how this restriction may change the universality class from the  $Z_n$  chiral clock model.

Fortuitously, the domain wall configurations for the  $n = 2$  case are unaffected. This is so because the two degenerate stripe patterns 001100, 100001 have exactly the same center of mass. As such, we expect the corresponding critical point to be in the universality class of the quantum Ising model in  $1+1$  dimensions. It predicts the following critical exponents:  $\nu = \nu z = 1$ ,  $\beta = 1/8$ . These are within 5–10% of the ones reported in Table I for the  $Z_2$  case.

In the  $Z_3$  case, we first compare our results with the three-state Potts model, which corresponds to the achiral  $Z_3$ -symmetry breaking transition in one dimension. It predicts  $\nu = \nu z = 5/6$ ,  $\beta = 1/9$ . While  $\nu$  and  $\beta$  are close to what we report in Table I,  $\nu z$  appears to be different. Since we

find the effective dynamical exponent  $z$  to be less than 1, the correlations travel faster compared to a light cone at long timescales and may be unphysical. This is similar to the  $Z_2$  case and we believe that it is affected by the assumption of SMA. Nevertheless, the dynamical exponent is significantly different from the chiral three-state clock model where  $z > 1$  [35–37]. A possible explanation is that our critical point is close to the achiral three-state Potts point and thus contains crossover physics. Or, as explained earlier in this section, the restriction on the domain wall configurations, due to the conservation law, changes the universality class away from the  $Z_3$  chiral clock model.

The achiral  $Z_4$  transition corresponds to a family of universality classes described by the Ashkin-Teller model and has continuously varying exponents. Our exponent  $\nu = 0.86$  suggests that the chiral perturbation would be relevant [38,39]. However, we note that the  $Z_4$  case is also affected by the same caveats as the  $Z_3$ -symmetry breaking transition.

## V. PHASE TRANSITION IN THE 2D LIMIT

The numerical results presented in this paper raise the interesting possibility of a continuous transition between a topologically ordered state and a conventional Landau ordered state, i.e., the stripe phase. At first sight, the two phases appear to be unrelated to one another. And the experience from Landau theory tells us that a direct transition between two unrelated conventionally ordered states is generally first order. As such, the nature of phase transitions that involve both the topological and Landau ordered states is an interesting problem. In this section, we argue that a continuous transition of the kind proposed in this paper can be understood within the framework of the composite-boson theory [20].

Composite bosons are emergent degrees of freedom obtained by attaching three flux quanta to electrons. We assume that the energy scale associated with Coulomb interactions is weak compared to the cyclotron energy. Therefore, the physics of the  $\nu_e = 7/3$  state is essentially equivalent to a filling fraction  $\nu_e = 2 + 1/3$ , i.e., a  $\nu_e = 1/3$  state with the Hamiltonian given by Eq. (1) and additional filled lowest LLs at  $\nu_e = 2$ . As such, we attach flux quanta only to the electrons residing in the partially filled  $N = 1$  LL. The isotropic case



can be described by the following Lagrangian:

$$\mathcal{L} = i\phi^* D_t^a \phi + \mu \phi^* \phi - \frac{1}{2m} \phi^* (D_j^a)^2 \phi + \frac{1}{12\pi} (a - A) d(a - A) + \frac{1}{2\pi} A dA \quad (10)$$

where  $\phi$ ,  $\phi^*$  are the composite-boson fields and  $D_\mu^a \equiv \partial_\mu - a_\mu$ .  $a_\mu$  and  $A_\mu$  are the emergent and electromagnetic gauge fields respectively and  $\mu$  corresponds to a chemical potential. The second to last term is the Chern-Simons term [40] with its prefactor signifying the three attached flux quanta. Additionally, the last term denotes the effect of the completely filled lowest LLs.

In the FQH side, the composite boson  $\phi$  condenses and forms a superfluid. The Goldstone mode of the superfluid is eaten up by the gauge field and one obtains the  $\nu_e = 7/3$  FQH state with gapped excitations. Importantly, the superfluid has a collective roton mode [41] which produces the magnetoroton excitation above the FQH state [20,25]. The transition to the stripe phase can take place if the roton condenses at a nonzero wave vector. The stripe phase would appear as coexisting superfluidity and the unidirectional CDW ordering. This is how a second-order transition could be allowed within a Landau theory framework.

We briefly note that the transition can also be understood from the perspective of composite-fermions (CFs) formed by attaching two flux quanta to electrons in the  $N = 1$  LL [42–46]. The  $\nu_e = 2 + 1/3$  filling fraction corresponds to a CF filling fraction  $\nu_{cf} = 1$ . As such, the stripe phase may be obtained by the condensation of the exciton excitation of CFs at a finite wave vector corresponding to a missing CF in the lowest CF LL and an extra CF in the first CF LL [47].

## VI. CONCLUSIONS

In this paper, we have presented evidence for a direct continuous phase transition from the Laughlin fractional quantum Hall (FQH) state at  $\nu_e = 7/3$  to a stripe ordered phase. The transition is found to take place as one makes the system anisotropic by introducing a band anisotropy.

We computed the correlation length, magnetoroton gap, and the stripe order parameter on an infinite cylinder

geometry and performed a critical scaling analysis. In a QH system on a cylinder, the translational symmetry is discrete and the stripe phase spontaneously breaks it “ $n$ -fold.” In the  $Z_2$  case, the exponents were found to be close to that of the quantum Ising model. However, for  $Z_3$  and  $Z_4$  cases, we find the exponents to be different compared to the chiral clock models, possibly due to the presence of the conservation of momentum along the circumference direction. Moreover, as one approaches the 2D limit by increasing the circumference, the effects of dislocations in the stripe order would become more important. These considerations suggest that the finite size scaling properties of the transition contain rich physics. We leave this as a problem to be addressed by future research.

Although the stripe and FQH states appear to be distinct, the theory of composite bosons provides a framework to study the critical point between the two. We argued that stripe phase can be understood as a coexistence phase of composite-boson superfluid and a Bose-Einstein condensate of the roton. The theory of this 2D quantum critical point is an interesting problem.

We note that the infinite cylinder geometry cannot distinguish between a smectic stripe phase and a stripe crystal [14]. The latter breaks translational symmetry in both  $x$  and  $y$  directions and the order along the circumference direction is hard to detect. If the FQH state goes into the stripe crystal in the 2D limit, as the anisotropy is increased, we expect it to do it via a first-order transition.

Experiments that study the effects of anisotropy are consistent with the emergence of a stripe order in the  $N = 1$  LL in the clean limit [48–53]. However, it is unclear whether they see a nematic or a stripe phase since the translational order is difficult to observe. We believe that measuring the magnetoroton dispersion at finite wave vectors may provide a more direct evidence of the stripe phase [54–58].

## ACKNOWLEDGMENTS

We thank Srinivas Raghu, Steve Kivelson, Matteo Ippoliti, and Hart Goldman for discussions. We thank the anonymous referee for providing insightful comments. The iDMRG numerical computations were carried out using the libraries developed by Roger Mong, Michael Zaletel and the TenPy Collaboration. This work was supported by DOE BES Grant No. DE-SC0002140.

- 
- [1] J. Maciejko, B. Hsu, S. A. Kivelson, Y. J. Park, and S. L. Sondhi, Field theory of the quantum Hall nematic transition, *Phys. Rev. B* **88**, 125137 (2013).
  - [2] Y. You, G. Y. Cho, and E. Fradkin, Theory of Nematic Fractional Quantum Hall States, *Phys. Rev. X* **4**, 041050 (2014).
  - [3] W. Pan, A. Serafin, J. S. Xia, L. Yin, N. S. Sullivan, K. W. Baldwin, K. W. West, L. N. Pfeiffer, and D. C. Tsui, Competing quantum Hall phases in the second Landau level in the low-density limit, *Phys. Rev. B* **89**, 241302(R) (2014).
  - [4] N. Samkharadze, K. A. Schreiber, G. C. Gardner, M. J. Manfra, E. Fradkin, and G. A. Csáthy, Observation of a transition from a topologically ordered to a spontaneously broken symmetry phase, *Nat. Phys.* **12**, 191 (2016).
  - [5] Y. You, G. Y. Cho, and E. Fradkin, Nematic quantum phase transition of composite fermi liquids in half-filled Landau levels and their geometric response, *Phys. Rev. B* **93**, 205401 (2016).
  - [6] N. Regnault, J. Maciejko, S. A. Kivelson, and S. L. Sondhi, Evidence of a fractional quantum Hall nematic phase in a microscopic model, *Phys. Rev. B* **96**, 035150 (2017).
  - [7] D. X. Nguyen, A. Gromov, and D. T. Son, Fractional quantum hall systems near nematicity: Bimetric theory, composite fermions, and Dirac brackets, *Phys. Rev. B* **97**, 195103 (2018).
  - [8] H. Wang, R. Narayanan, X. Wan, and F. Zhang, Fractional quantum Hall states in two-dimensional electron systems with anisotropic interactions, *Phys. Rev. B* **86**, 035122 (2012).

- [9] B. Yang, Z. Papić, E. H. Rezayi, R. N. Bhatt, and F. D. M. Haldane, Band mass anisotropy and the intrinsic metric of fractional quantum Hall systems, *Phys. Rev. B* **85**, 165318 (2012).
- [10] E. H. Rezayi and F. D. M. Haldane, Incompressible Paired Hall State, Stripe Order, and the Composite Fermion Liquid Phase in Half-Filled Landau Levels, *Phys. Rev. Lett.* **84**, 4685 (2000).
- [11] W. N. Faugno, T. Zhao, A. C. Balram, T. Jolicoeur, and J. K. Jain, Unconventional  $\mathbb{Z}_n$  parton states at  $\nu = 7/3$ : Role of finite width, *Phys. Rev. B* **103**, 085303 (2021).
- [12] A. A. Koulakov, M. M. Fogler, and B. I. Shklovskii, Charge Density Wave in Two-Dimensional Electron Liquid in Weak Magnetic Field, *Phys. Rev. Lett.* **76**, 499 (1996).
- [13] M. M. Fogler, A. A. Koulakov, and B. I. Shklovskii, Ground state of a two-dimensional electron liquid in a weak magnetic field, *Phys. Rev. B* **54**, 1853 (1996).
- [14] E. Fradkin and S. A. Kivelson, Liquid-crystal phases of quantum Hall systems, *Phys. Rev. B* **59**, 8065 (1999).
- [15] Z. Papić, Fractional quantum Hall effect in a tilted magnetic field, *Phys. Rev. B* **87**, 245315 (2013).
- [16] Z. Zhu, I. Sodemann, D. N. Sheng, and L. Fu, Anisotropy-driven transition from the Moore-Read state to quantum Hall stripes, *Phys. Rev. B* **95**, 201116(R) (2017).
- [17] Y. He, K. Yang, M. O. Goerbig, and R. S. K. Mong, Charge density waves and their transitions in anisotropic quantum Hall systems, *Commun. Phys.* **4**, 116 (2021).
- [18] I. P. McCulloch, Infinite size density matrix renormalization group, revisited, [arXiv:0804.2509](https://arxiv.org/abs/0804.2509).
- [19] M. P. Zaletel, R. S. K. Mong, F. Pollmann, and E. H. Rezayi, Infinite density matrix renormalization group for multicomponent quantum Hall systems, *Phys. Rev. B* **91**, 045115 (2015).
- [20] S. C. Zhang, T. H. Hansson, and S. Kivelson, Effective-Field-Theory Model for the Fractional Quantum Hall Effect, *Phys. Rev. Lett.* **62**, 82 (1989).
- [21] A. Krishna, F. Chen, M. Ippoliti, and R. N. Bhatt, Interaction-dependent anisotropy of fractional quantum Hall states, *Phys. Rev. B* **100**, 085129 (2019).
- [22] B. A. Bernevig and F. D. M. Haldane, Model Fractional Quantum Hall States and Jack Polynomials, *Phys. Rev. Lett.* **100**, 246802 (2008).
- [23] E. J. Bergholtz and A. Karlhede, Quantum Hall system in Tao-Thouless limit, *Phys. Rev. B* **77**, 155308 (2008).
- [24] U. Schollwöck, The density-matrix renormalization group in the age of matrix product states, *Ann. Phys. (NY)* **326**, 96 (2011).
- [25] S. M. Girvin, A. H. MacDonald, and P. M. Platzman, Magnetoroton theory of collective excitations in the fractional quantum Hall effect, *Phys. Rev. B* **33**, 2481 (1986).
- [26] One such possible interaction can be between the magnetoroton at wave vector  $\mathbf{G}$  and the state composed of three-rotons with a total momentum  $\mathbf{q} = \mathbf{q}_1 + \mathbf{q}_2 + \mathbf{q}_3 = \mathbf{G}$ , where  $\mathbf{q}_1 = \mathbf{q}_2 = -\mathbf{q}_3 = \mathbf{G}$ . Nevertheless, the SMA energy has a physical meaning as it is equal to the average energy of excitations weighted by the dynamical structure factor [25]. As long as the spectral weight of critical fluctuations diverges, it should capture the dynamical properties of critical fluctuations.
- [27] We fit the data using the linear least squares error method. We have modified the algorithm by including weights proportional to the square of the observables. As long as the difference between the fitted curve and the data is small, this modification effectively corresponds to a linear least square error algorithm on a log-log scale.
- [28] By effective exponents, we mean the exponents obtained by fitting the data in the parameter regime accessible to our numerics. In general, the data may contain irrelevant corrections from scales such as the cylinder circumference  $L_x$ , interaction range  $\xi$ , bond dimension  $\chi$ , and proximity to other critical points such as the achiral Potts model. On the other hand, the asymptotic exponents correspond to the limit in which these corrections vanish. To determine how close our effective exponents are to the asymptotic ones requires going closer to the critical point and bigger bond dimensions than we are currently able to.
- [29] In addition, ground state at each anisotropy on the FQH side was obtained in an independent simulation as opposed to the adiabatic evolution method mentioned in Sec. II A.
- [30] S. Ostlund, Incommensurate and commensurate phases in asymmetric clock models, *Phys. Rev. B* **24**, 398 (1981).
- [31] D. A. Huse and M. E. Fisher, Domain Walls and the Melting of Commensurate Surface Phases, *Phys. Rev. Lett.* **49**, 793 (1982).
- [32] P. Fendley, Parafermionic edge zero modes in  $\mathbb{Z}_n$ -invariant spin chains, *J. Stat. Mech.* (2012) P11020.
- [33] Y. Zhuang, H. J. Changlani, N. M. Tubman, and T. L. Hughes, Phase diagram of the  $\mathbb{Z}_3$  parafermionic chain with chiral interactions, *Phys. Rev. B* **92**, 035154 (2015).
- [34] S. Whitsitt, R. Samajdar, and S. Sachdev, Quantum field theory for the chiral clock transition in one spatial dimension, *Phys. Rev. B* **98**, 205118 (2018).
- [35] R. Samajdar, S. Choi, H. Pichler, M. D. Lukin, and S. Sachdev, Numerical study of the chiral  $\mathbb{Z}_3$  quantum phase transition in one spatial dimension, *Phys. Rev. A* **98**, 023614 (2018).
- [36] N. Chepiga and F. Mila, Floating Phase versus Chiral Transition in a 1D Hard-Boson Model, *Phys. Rev. Lett.* **122**, 017205 (2019).
- [37] S. Nyckees, J. Colbois, and F. Mila, Identifying the Huse-Fisher universality class of the three-state chiral Potts model, *Nucl. Phys. B* **965**, 115365 (2021).
- [38] H. J. Schulz, Phase transitions in monolayers adsorbed on uniaxial substrates, *Phys. Rev. B* **28**, 2746 (1983).
- [39] N. Chepiga and F. Mila, Kibble-Zurek exponent and chiral transition of the period-4 phase of Rydberg chains, *Nat. Commun.* **12**, 414 (2021).
- [40]  $adb$  is a shorthand for  $\epsilon^{\mu\nu\lambda} a_\mu \partial_\nu a_\lambda$ .
- [41] R. P. Feynman, *Statistical Mechanics: A Set of Lectures* (Westview, Boulder, 1998), Chap. 11.
- [42] J. K. Jain, Composite-Fermion Approach for the Fractional Quantum Hall Effect, *Phys. Rev. Lett.* **63**, 199 (1989).
- [43] A. Lopez and E. Fradkin, Fractional quantum Hall effect and Chern-Simons gauge theories, *Phys. Rev. B* **44**, 5246 (1991).
- [44] V. Kalmeyer and S.-C. Zhang, Metallic phase of the quantum Hall system at even-denominator filling fractions, *Phys. Rev. B* **46**, 9889 (1992).
- [45] B. I. Halperin, P. A. Lee, and N. Read, Theory of the half-filled Landau level, *Phys. Rev. B* **47**, 7312 (1993).
- [46] J. Y. Lee, C. Wang, M. P. Zaletel, A. Vishwanath, and Y.-C. He, Emergent Multi-Flavor QED<sub>3</sub> at the Plateau Transition between Fractional Chern Insulators: Applications to Graphene Heterostructures, *Phys. Rev. X* **8**, 031015 (2018).
- [47] J. K. Jain, *Composite Fermions* (Cambridge University Press, Cambridge, 2007).
- [48] W. Pan, R. R. Du, H. L. Stormer, D. C. Tsui, L. N. Pfeiffer,

- K. W. Baldwin, and K. W. West, Strongly Anisotropic Electronic Transport at Landau Level Filling Factor  $\nu = 9/2$  and  $\nu = 5/2$  under a Tilted Magnetic Field, *Phys. Rev. Lett.* **83**, 820 (1999).
- [49] W. Pan, J. Xia, E. Adams, R. Du, H. Stormer, D. Tsui, L. Pfeiffer, K. Baldwin, and K. West, New results at half-fillings in the second and third Landau level, *Physica B* **298**, 113 (2001).
- [50] C. R. Dean, B. A. Piot, P. Hayden, S. Das Sarma, G. Gervais, L. N. Pfeiffer, and K. W. West, Contrasting Behavior of the  $\frac{5}{2}$  and  $\frac{7}{3}$  Fractional Quantum Hall Effect in a Tilted Field, *Phys. Rev. Lett.* **101**, 186806 (2008).
- [51] J. Xia, V. Cvicek, J. P. Eisenstein, L. N. Pfeiffer, and K. W. West, Tilt-Induced Anisotropic to Isotropic Phase Transition at  $\nu = 5/2$ , *Phys. Rev. Lett.* **105**, 176807 (2010).
- [52] J. Xia, J. P. Eisenstein, L. N. Pfeiffer, and K. W. West, Evidence for a fractionally quantized Hall state with anisotropic longitudinal transport, *Nat. Phys.* **7**, 845 (2011).
- [53] Y. Liu, S. Hasdemir, M. Shayegan, L. N. Pfeiffer, K. W. West, and K. W. Baldwin, Evidence for a  $\nu = 5/2$  fractional quantum Hall nematic state in parallel magnetic fields, *Phys. Rev. B* **88**, 035307 (2013).
- [54] M. Kang, A. Pinczuk, B. S. Dennis, L. N. Pfeiffer, and K. W. West, Observation of Multiple Magnetorotons in the Fractional Quantum Hall Effect, *Phys. Rev. Lett.* **86**, 2637 (2001).
- [55] T. D. Rhone, D. Majumder, B. S. Dennis, C. Hirjibehedin, I. Dujovne, J. G. Groshaus, Y. Gallais, J. K. Jain, S. S. Mandal, A. Pinczuk, L. Pfeiffer, and K. West, Higher-Energy Composite Fermion Levels in the Fractional Quantum Hall Effect, *Phys. Rev. Lett.* **106**, 096803 (2011).
- [56] U. Wurstbauer, A. L. Levy, A. Pinczuk, K. W. West, L. N. Pfeiffer, M. J. Manfra, G. C. Gardner, and J. D. Watson, Gapped excitations of unconventional fractional quantum Hall effect states in the second Landau level, *Phys. Rev. B* **92**, 241407(R) (2015).
- [57] L. Du, U. Wurstbauer, K. W. West, L. N. Pfeiffer, S. Fallahi, G. C. Gardner, M. J. Manfra, and A. Pinczuk, Observation of new plasmons in the fractional quantum Hall effect: Interplay of topological and nematic orders, *Sci. Adv.* **5**, eaav3407 (2019).
- [58] Z. Liu, U. Wurstbauer, L. Du, K. W. West, L. N. Pfeiffer, M. J. Manfra, and A. Pinczuk, Domain Textures in the Fractional Quantum Hall Effect, *Phys. Rev. Lett.* **128**, 017401 (2022).